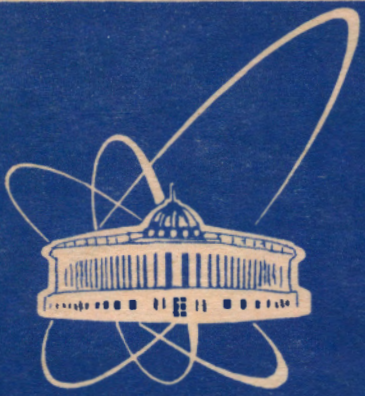

ОБЪЕДИНЕННЫЙ
ИНСТИТУТ
ЯДЕРНЫХ
ИССЛЕДОВАНИЙ

Дубна

E17-96-466

V.O.Nesterenko, W.Kleinig[1]

RPA DESCRIPTION OF DIPOLE OSCILLATIONS IN DEFORMED SODIUM CLUSTERS

Submitted to «Physical Review B»

[1]Technical University of Dresden, Institute for Analysis, D-01062, Dresden, Germany

1996

1 Introduction

Collective oscillations in metal clusters are a subject of intensive experimental and theoretical investigations during the last decade (see reviews [1-5] as well as some recent papers on the theory [6-16] and experiment [17-22]). Most of the theoretical studies cover spherical clusters while only a few are devoted to deformed ones [6,8,13,15,23]. The latter is caused by a considerable computational effort which one needs for deformed clusters. In this case, the configurational particle-hole space is very extended and we have to diagonalize RPA matrices of high rank. To overcome this trouble, the RPA method with the self-consistent separable residual forces (SRPA) has been proposed [8,13-16]. Otherwise this method is called the vibrating potential model. The SRPA exploits the separable ansatz which in a familiar convention [24-26] means the factorization of a two-body interaction through the single-particle matrix elements: $\sum_{p_1,p_2,h_2,h_1} V(p_1,p_2,h_2,h_1) = \kappa \sum_{p_1,p_2,h_2,h_1} q(p_1,h_1)q(p_2,h_2)$ where $q(p_1,h_1)$ are the single-particle (particle-hole) matrix elements of one-body operators. The separable ansatz allows one to turn the RPA matrix into a dispersion relation which drastically simplifies the eigenvalue problem. At the same time, the SRPA enables us to treat the Landau damping as in a full RPA [6,7,9-11].

The SRPA is especially attractive since, due to the consistency between time-dependent variations of the single-particle potential and density, it provides expressions for the strength constant κ and one-body operators of the separable residual forces. So, this method does not need any adjusting parameters. First application of the SRPA to spherical and deformed sodium clusters has demonstrated good perspectives of this model [14,15]. Quite recently the SRPA has been modified to take into account the coupling of surface and volume dipole modes, and totally self-consistent calculations have been performed for neutral and singly charged spherical

sodium clusters in a wide size region [16]. Good agreement of the calculated characteristics (dipole plasmon energies, Landau damping, static dipole polarizabilities, main tendencies with increasing a cluster size) with available experimental data has been achieved, which strictly testifies to the validity of the separable ansatz for sodium clusters.

In this investigation, we present the SRPA results for dipole oscillations in axially *deformed* singly charged sodium clusters Na_{11}^+, Na_{15}^+, Na_{27}^+ and Na_{35}^+ for which the precise photoabsorption experimental data have been recently obtained [18,22,27]. These clusters include the patterns of prolate and oblate forms as well as of large hexadecapole deformation (see Table 1 below). In addition to [15], the coupling of surface and volume modes is taken into account. This coupling was shown to considerably improve the description of high-energy dipole strength [16]. Also, the coupling of dipole and octupole excitations, a particular property of deformed systems, is included. The larger deformation, the stronger this effect. Since some sodium clusters possess very large quadrupole deformation, the investigation of the dipole-octupole coupling is quite desirable.

The SRPA results will be shown to be in good agreement with the experimental data, thus providing encouraging perspectives of this model for a description of dipole oscillations in deformed clusters.

2 Main SRPA equations

A sketch of the SRPA will first be presented (for details see ref. [16]). Starting with the Kohn-Sham density-dependent equations (with the jellium approximation for ions) and considering the density of valence electrons as a sum of the static ground-state density and small time-dependent variation, $n(\mathbf{r},t) = n_{gr}(\mathbf{r}) + \delta n(\mathbf{r},t)$, one separates a time-dependent single-particle potential into static and dynamic parts

$$H(\mathbf{r},t) = T + V_0(\mathbf{r}) + \delta H(\mathbf{r},t) \qquad (1)$$

where the latter is

$$\delta H(\mathbf{r},t) = (\frac{d^2v}{dn^2})_{n=n_{gr}} \delta n(\mathbf{r},t) + \int \frac{\delta n(\mathbf{r_1},t)}{|\mathbf{r}-\mathbf{r_1}|} d\mathbf{r_1}. \qquad (2)$$

Here, $v(n(\mathbf{r}))$ is the exchange-correlation term in the local density approximation [28], $n_{gr}(\mathbf{r}) = \Sigma_l |\phi_l(\mathbf{r})|^2$ is the ground state density, $\phi_l(\mathbf{r})$ is the single-particle wave function. In the present paper, the static single-particle potential $V_0(\rho(\mathbf{r}),\mathbf{r})$ is approximated by the phenomenological Woods-Saxon potential and the density $n_{gr}(\mathbf{r})$ is calculated through the Woods-Saxon single-particle wave functions.

The perturbed time-dependent wave function of the system is defined through the scaling transformation

$$\Psi_j(\mathbf{r}_1,...,\mathbf{r}_{N_e},t) = \prod_{k=1}^{K} e^{i\alpha_{\lambda\mu k}^j(t)\sum_{i=1}^{N_e}[H_0(\mathbf{r}_i),f_{\lambda\mu k}(\mathbf{r}_i)]} \Psi_0(\mathbf{r}_1,...,\mathbf{r}_{N_e}), \qquad (3)$$

where Ψ_0 is the ground-state wave function ($H_0\Psi_0 = 0$) and j labels the number of the excited state. Both Ψ_0 and Ψ_j are the Slater determinants. The local hermitian coordinate operators $f_{\lambda\mu k}(\mathbf{r})$ determine the kinds of collective motion provided by the density variation. They influence the eigenstates and eigenenergies of the system and should not be confused with an external field operator. For the reasons given below, these operators are chosen as

$$f_{\lambda\mu k}(\mathbf{r}) = r^{p_k}(Y_{\lambda\mu}(\theta,\phi) + Y_{\lambda\mu}^{\dagger}(\theta,\phi)) \qquad (4)$$

with $k = 1,...,K$. Further, $\alpha_{\lambda\mu k}^j(t) = \alpha_{\lambda\mu k}^{j0} cos(\omega t)$ are the harmonic collective variables. Their normalized amplitudes $\alpha_{\lambda\mu k}^{j0}$ are calculated from the final SRPA equations.

In virtue of eq. (4), the density variation can be written in the form

$$\delta n_j(\mathbf{r},t) = \sum_{k=1}^{K} \alpha_{\lambda\mu k}^j(t)(\nabla n_{gr}(\mathbf{r}) \cdot \nabla f_{\lambda\mu k}(\mathbf{r}) + n_{gr}(\mathbf{r}) \triangle f_{\lambda\mu k}(\mathbf{r})). \qquad (5)$$

It is seen to include both surface $\sim \nabla n_{gr}(\mathbf{r})$ and volume $\sim n_{gr}(\mathbf{r})$ terms. If $p_k = \lambda$, we have a divergency-free operator ($\triangle f_{\lambda\mu k}(\mathbf{r}) = 0$), and eq. (5) has

only the surface term. This case has been considered in [15]. The operators with $p_k > \lambda$ are responsible for a volume collective motion: they shift the maximum of the density variation towards the interior of the system. The volume degrees of freedom for dipole excitations are important in both atomic nuclei and metal clusters [16,29,30,32,33]. Three groups of local operators $f_{\lambda\mu k}(\mathbf{r}) = r^{p_k}(Y_{\lambda\mu}(\theta,\phi) + Y^{\dagger}_{\lambda\mu}(\theta,\phi))$ are used in the present paper for every projection μ: a) $\lambda p_k = 11$ (dipole mode of surface character), b) $\lambda p_k = 13, 15$ (dipole modes of volume character), c) $\lambda p_k = 33, 35$ (octupole modes).

Substituting (1) into time-dependent Hartree-Fock equation and following the standard procedures [8,13-16], one finally gets the system of homogeneous equations to determine the amplitudes $\alpha^{j0}_{\lambda\mu k}$:

$$\sum_{k'=1}^{K} S_{\lambda\mu kk'}(\omega)\alpha^{j0}_{\lambda\mu k'} = 0 \qquad (6)$$

with

$$S_{\lambda\mu kk'}(\omega) = \sum_{ph} \frac{< p|Q_{\lambda\mu k}|h >< p|Q_{\lambda\mu k'}|h > \epsilon_{ph}}{\epsilon^2_{ph} - \omega^2} - \frac{1}{2\kappa_{\lambda\mu kk'}}. \qquad (7)$$

The condition

$$det \mid S_{\lambda\mu kk'}(\omega) \mid = 0 \qquad (8)$$

provides non-trivial solutions to the system (6) and represents the SRPA dispersion equation for eigenenergies ω_j where j is the number of the root of equation (8).

In eq.(7),

$$Q_{\lambda\mu k}(\mathbf{r}) = (\frac{d^2v}{dn^2})_{n=n_{gr}} \cdot (\nabla n_{gr}(\mathbf{r}) \cdot \nabla f_{\lambda\mu k}(\mathbf{r}) + n_{gr}(\mathbf{r}) \triangle f_{\lambda\mu k}(\mathbf{r}))$$
$$+ \int \frac{(\nabla n_{gr}(\mathbf{r}_1) \cdot \nabla f_{\lambda\mu k}(\mathbf{r}_1) + n_{gr}(\mathbf{r}_1) \triangle f_{\lambda\mu k}(\mathbf{r}_1))}{|\mathbf{r} - \mathbf{r}_1|} d\mathbf{r}_1 \qquad (9)$$

is the self-consistent operator of the residual interaction and

$$\kappa^{-1}_{\lambda\mu kk'} = -\int Q_{\lambda\mu k}(\mathbf{r})(\nabla n_{gr}(\mathbf{r}) \cdot \nabla f_{\lambda\mu k'}(\mathbf{r}) + n_{gr}(\mathbf{r}) \triangle f_{\lambda\mu k'}(\mathbf{r}))d\mathbf{r} \qquad (10)$$

is the inverse strength constant of this interaction. If more than one local operator is used, the nondiagonal strength constants take place, which regulate in a self-consistent way the Hamiltonian after adding a new interaction.

It is worth comparing the SRPA with other RPA methods used for description of the dipole plasmon in deformed clusters. This is first the local RPA [4,12,29-31] which, being based on K input local operators, represents the system of K coupled harmonical oscillators. By analogy with the local RPA, the SRPA with K local operators represents the system of K coupled RPA motions. However, the local RPA has K RPA solutions (usually $K = 3 \div 10$) and can describe only gross-structure of the collective strength, while the SRPA gives much more RPA roots (their number is determined by the particle-hole basis) and can successfully describe not only gross-structure but also the Landau damping. The principle point is that, unlike full RPA methods [6,7,9-11], the SRPA does not need for this aim a huge computational effort. Indeed, due to the separable ansatz the rank of the matrix (7) is much smaller than the rank of the matrices in the full RPA methods, which drastically simplifies the RPA calculations.

The connection of the SRPA with the familiar separable RPA is quite evident in the case of one local operator. Then, the dispersion equation (8) is reduced to the well-known equation $S_{\lambda\mu}(\omega) = 0$ [24,26]. The same dispersion equation would take place if we start with the Hamiltonian containing the separable residual interaction $H_{\lambda\mu} = H_0 - \frac{1}{2}\kappa_{\lambda\mu}Q^{\dagger}_{\lambda\mu}Q_{\lambda\mu}$.

Neglecting the direct Coulomb terms in the SRPA, one gets the model for the self-consistent description of isoscalar collective excitations (giant resonances) in atomic nuclei. Quite recently this model was successfully applied to describe isoscalar $E\lambda$ giant resonances in deformed and superdeformed nuclei [34].

For deformed clusters it is convenient to use the multiple expansion of

the ground state density $n_{gr}(\mathbf{r}) = 2\Sigma_{lm} n_l(r)Y_{l0}(\theta)$. Then, using (4), the operator (9) is written as

$$Q_{\lambda\mu k}(\mathbf{r}) = \sum_{LM} Y_{LM}(\theta) \sum_{lm} Q^{(k)}_{\lambda\mu Llm}(r) \tag{11}$$

where

$$Q^{(k)}_{\lambda\mu Llm}(r) = -\frac{2}{\sqrt{4\pi(2L+1)}}(C^{LM}_{lm\lambda\mu} + (-1)^{\mu} C^{LM}_{lm\lambda-\mu})\{(\frac{d^2v}{dn^2})_{n=n_{gr}} R^{(k)}_{\lambda Ll}(r)$$

$$+ \frac{4\pi}{2L+1}[r^{-(L+1)} \int_0^r R^{(k)}_{\lambda Ll}(r_1) r_1^{L+2} dr_1 + r^L \int_r^{\infty} R^{(k)}_{\lambda Ll}(r_1) r_1^{-(L-1)} dr_1]\} \tag{12}$$

and

$$R^{(k)}_{\lambda Ll}(r) = r^{p_k - 1}\{\frac{dn_l(r)}{dr} N^{(k)}_{\lambda Ll} + \frac{n_l(r)}{r} M^{(k)}_{\lambda Ll}\}. \tag{13}$$

Here, $C^{LM}_{lm\lambda\mu}$ is the Clebsch-Gordan coefficient. Expressions for $N^{(k)}_{\lambda Ll}$ and $M^{(k)}_{\lambda Ll}$ are given in the Appendix.

Expression (12) shows that the coupling of the excitation of multipolarity λ with the spherical ($l = 0$) and deformed ($l = 2, 4, 6, ...$) parts of the single-particle potential (and density) leads to the appearance in the residual interaction of a family of modes with the moments $\mid \lambda - l \mid \leq L \leq \lambda + l$ and the parity $(-1)^{\lambda}$. Due to the consistency between $\delta n(\mathbf{r}, t)$ and $\delta H(\mathbf{r}, t)$, the residual interaction takes into account all the deformation distortions of the static single-particle potential $V_0(\mathbf{r})$ and ground-state density $n_{gr}(\mathbf{r})$.

3 Results and discussion

As has been mentioned above, in the present study the static single-particle potential $V_0(\rho(\mathbf{r}))$ is approximated by the phenomenological Woods-Saxon potential

$$V_{WS}(\mathbf{r}) = \frac{V_0}{(1 + exp[(r - R(\theta)/a_0])} \tag{14}$$

where $R(\theta) = R_0(1 + \beta_0 + \beta_2 Y_{20}(\theta) + \beta_4 Y_{40}(\theta))$, $R_0 = r_0 N^{1/3}$, N is the number of atoms in the cluster (for singly charged clusters $N = N_e - 1$), β_2 and β_4 are the parameters of quadrupole and hexadecapole deformation, the parameter β_0 ensures the conservation of the cluster volume. The parameters of the potential ($r_0 = 2.5\AA$, $V_0 = -7.2$ eV and $a_0 = 1.25\AA$) for

Table 1: Deformation parameters β_2 and β_4 (experimental [18,22,27] and calculated within the SAJM [35]) and diagonal elements of the inertia tensor Θ_z and Θ_x (calculated within the SAJM [35,36] and with the Woods-Saxon potential containing the deformation parameters from [35]). See comments in the text.

	Exp.[18]	Exp.[22,27]	SAJM [35]		SAJM [35,36]		WS	
Cluster	β_2	β_2	β_2	β_4	Θ_z	Θ_x	Θ_z	Θ_x
Na^+_{11}	-	0.38	0.384	0.234	0.70	1.15	0.68	1.16
Na^+_{15}	0.32	0.32	0.56	-0.14	0.68	1.16	0.65	1.18
Na^+_{27}	0.23	0.21	0.37	0.11	0.74	1.13	0.72	1.14
Na^+_{35}	-0.23	-0.23	-0.27	0.03	1.15	0.93	1.16	0.92

singly charged clusters have been adjusted in [16] so as to reproduce on average the Kohn-Sham (with diffused jellium) ground state densities in a wide size region. Using these parameters, the description of dipole oscillations of the same quality as in the case of the Kohn-Sham single-particle scheme has been achieved. The deformation parameters β_2 and β_4 have been taken from the calculations within the Structure-Averaged Jellium Model (SAJM) [35] and extracted from the measured deformation splitting of the dipole plasmon [18,22,27] following the prescription of ref.[35]. These parameters are given in Table 1. It is seen that the SAMJ β_2 values are systematically larger than the experimental ones (see comments in [35]). Before using the SAJM deformation parameters in the Woods-Saxon potential, we have checked the validity of this application by calculating dimensionless diagonal elements of the inertia tensor $\Theta_j = \int (r^2 - x_j^2) n_{gr}(\mathbf{r}) d\mathbf{r}$ (with $j = x, z$ and normalization condition $\Sigma_{j=x,y,z} \Theta_j = 3$) and comparing them with the corresponding SAJM values obtained for valence electrons [36] (see Table 1). The good agreement obtained certainly testifies to the applicability of the SAJM deformation parameters in the Woods-Saxon potential. The comparison of the calculated quadrupole and hexadecapole moments confirms this conclusion.

The main results of our calculations are presented in Table 2 and Figures

1-6. In the figures the strength function

$$\sigma(E\lambda,\omega) = \sum_j \omega_j B(E\lambda, gr \to \omega_j)\rho(\omega - \omega_j)/S\,(E\lambda 1) \qquad (15)$$

normalized to the energy-weighted sum rule

$$S(E\lambda) = \sum_j \omega_j B(E\lambda, gr \to \omega_j) = \frac{\hbar^2 e^2}{8\pi m_e}\lambda(2\lambda+1)^2 N < r^{2\lambda-2} > \qquad (16)$$

and averaged by the weight function

$$\rho(\omega - \omega_j) = \frac{1}{2\pi}\frac{\Delta}{(\omega-\omega_j)^2 + (\Delta/2)^2} \qquad (17)$$

is presented. In (15)-(17), $B(E\lambda, gr \to \omega_j)$ is the reduced probability of the $E\lambda$ transition from the ground state to the one-phonon state with the excitation energy ω_j, Δ is the averaging parameter. Expression (15) has a form similar to the photo-absorption cross section for dipole excitations. However, this is not exactly the photo-absorption cross section but only a convenient form of presentation of the RPA results where the values $\omega_j B(E\lambda, gr \to \omega_j)$ are averaged to avoid unnecessary details.

In Figs. 1-4, the strength functions for dipole oscillations are given for three cases: a) only surface mode ($\lambda p_k = 11$), b) surface and volume modes ($\lambda p_k = 11, 13, 15$), c) surface and volume modes as well as the coupling with octupole modes ($\lambda p_k = 11, 13, 15, 33, 35$). The physical ground for these modes has been discussed in Section 2. As compared with the previous calculations for deformed clusters [15], the couplings with volume and octupole modes are added, the optimized parameters of the Wood-Saxon potential are used and the Gunnarsson-Lundqvist prescription for the exchange-correlation term is exploited.

As is seen from Figs. 1-4, the dipole plasmon exhibits deformation splitting into $\mu = 0$ and $\mu = 1$ parts. The coupling of the surface and volume modes considerably changes the description. It influences the position and fragmentation of the plasmon and redshifts the high-energy dipole strength. The latter is especially important for clusters with $N_e > 20$

where the calculations with surface forces only ($\lambda p_k = 11$) overestimate the high-energy dipole strength (see also [15,16]). The influence of the coupling with octupole modes turns out to be negligible in all clusters. including strongly deformed Na_{11}^+ and Na_{15}^+. The effect of hexadecapole deformation considered in Na_{11}^+, the cluster with very large hexadecapole deformation ($\beta_4 = 0.234$), is more noticeable. If the hexadecapole deformation is neglected, the $\mu = 0$ peak is splitted and the $\mu = 1$ peak is redshifted by about 0.1 eV. Starting with Na_{15}^+, the calculations demonstrate large fragmentation (Landau damping) of right plasmon peaks. which should considerably contribute to the plasmon widths. The plasmon peaks at 2-3.5 eV are mainly of surface character while the peaks at 5 eV represent very fragmented volume plasmon.

Figs. 5 and 6 compare the experimental data [22,27] with the SRPA results obtained for the maximal set of local operators ($\lambda p_k = 11, 13, 15, 33, 35$) when both surface-volume coupling and influence of octupole excitations are taken into account. The strength functions with the small ($\Delta = 0.05eV$) and large ($\Delta = 0.25eV$) averaging are presented. The large averaging simulates the thermal widening of the plasmon and makes easier the comparison of the theoretical and experimental results. For example, in Na_{27}^+ just the large averaging allows one to demonstrate the correct ratio between left and right peaks obtained in the calculations. Figs. 5 and 6 exhibit the SRPA results obtained with the deformation parameters calculated within the SAJM and extracted from the experimental data [22,27]. In the first case, the calculated deformation splitting of the dipole plasmon is considerably overestimated (see also Table 2) while in the second one it is described quite well. It is seen that in general the SRPA results are in good agreement with the experimental data. Comparison of the strength functions with a small and large averaging demonstrate an important role of the Landau damping in forming the plasmon width in deformed clusters starting with Na_{15}^+. Due to the Landau damping, the ratios between peaks and such details as a strong high-energy-side shoulder of the right peaks in Na_{15}^+ - Na_{35}^+ and mainly one-peak structure of the plasmon in oblate Na_{35}^+ are well described.

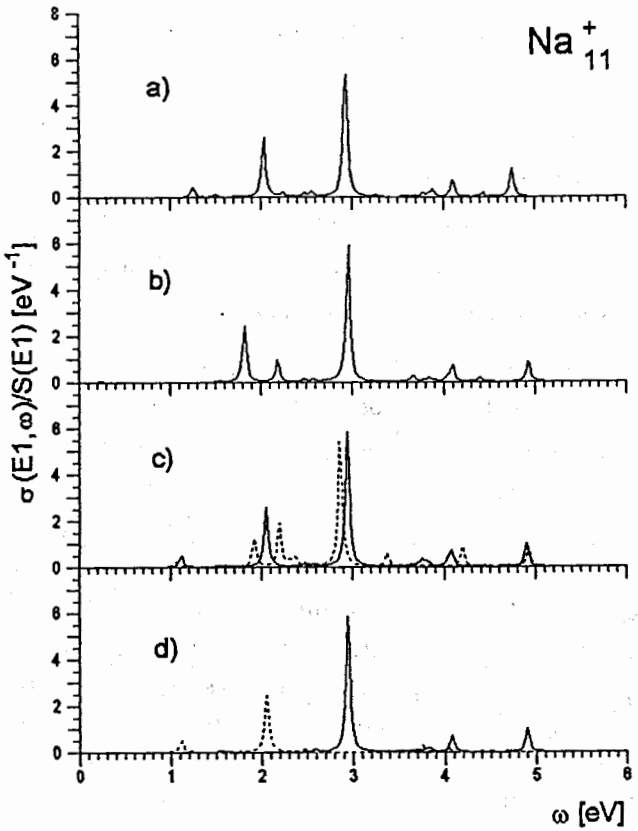

Fig. 1. Normalized E1 strength functions calculated for Na_{11}^{+} within the SRPA for the cases of: a) surface mode ($\lambda p_k = 11$), b) surface and volume modes ($\lambda p_k = 11, 13, 15$), c) surface and volume modes as well as the coupling with octupole excitations ($\lambda p_k = 11, 13, 15, 33, 35$). On the panel c) the strength function with $\beta_4 = 0$ is also presented (dashed curve). The panel d) contains separate $\mu = 0$ (dashed curve) and $\mu = 1$ (solid curve) components of the strength function. The SAJM deformation parameters [35] and the averaging parameter $\Delta = 0.05eV$ are used.

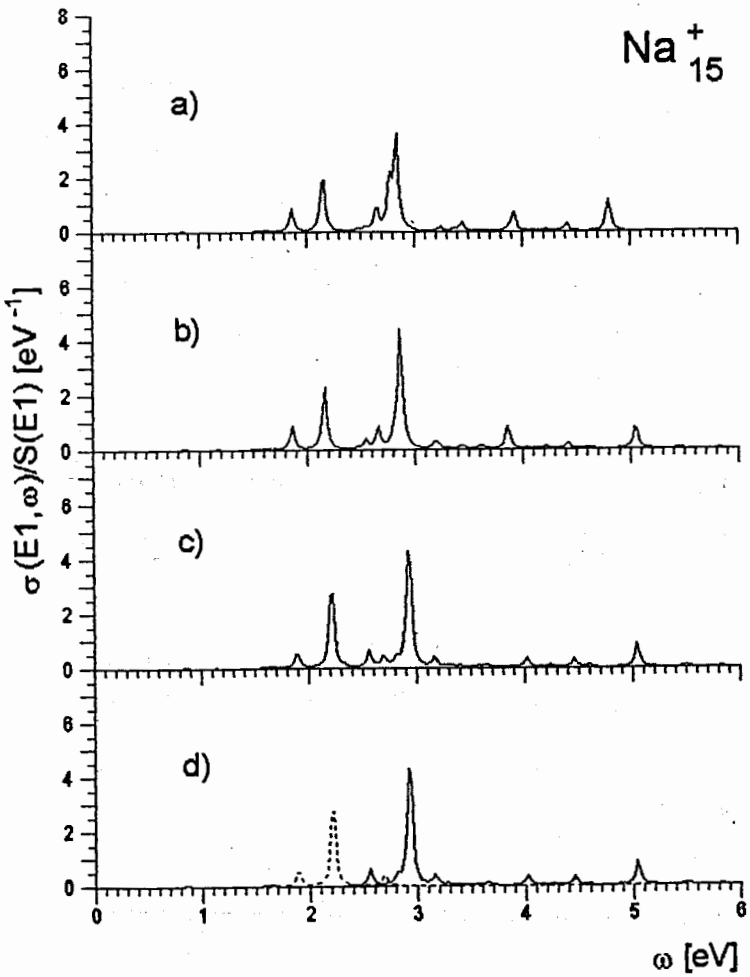

Fig.2. The same as in Fig. 1 (except for the case with $\beta_4 = 0$) for Na_{15}^{+}.

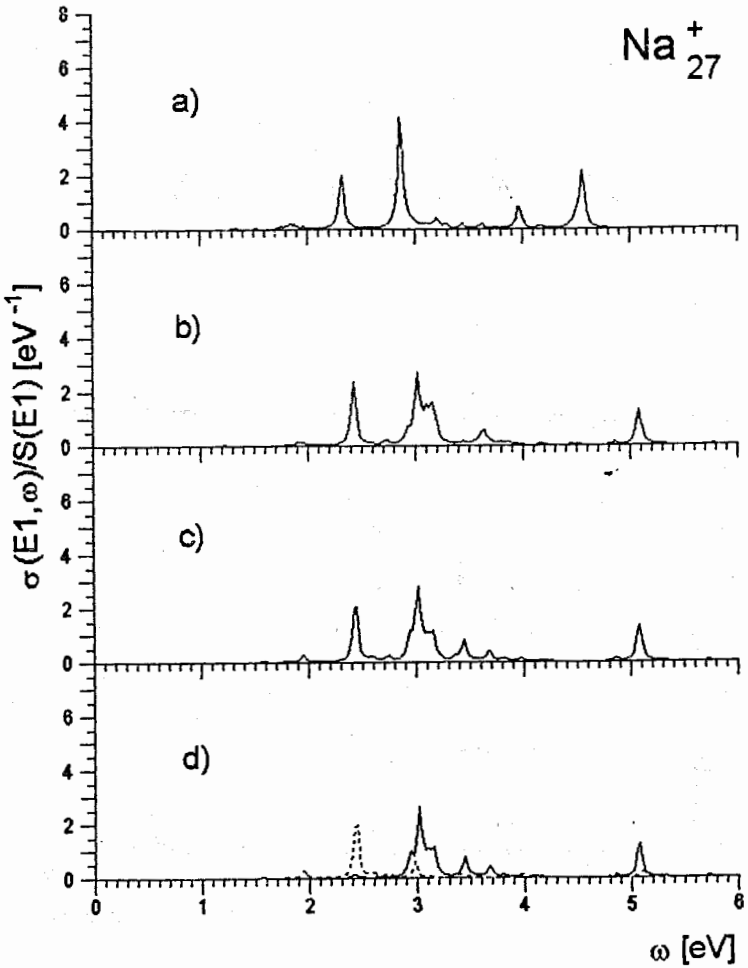

Fig.3. The same as in Fig. 2 for Na_{27}^{+}.

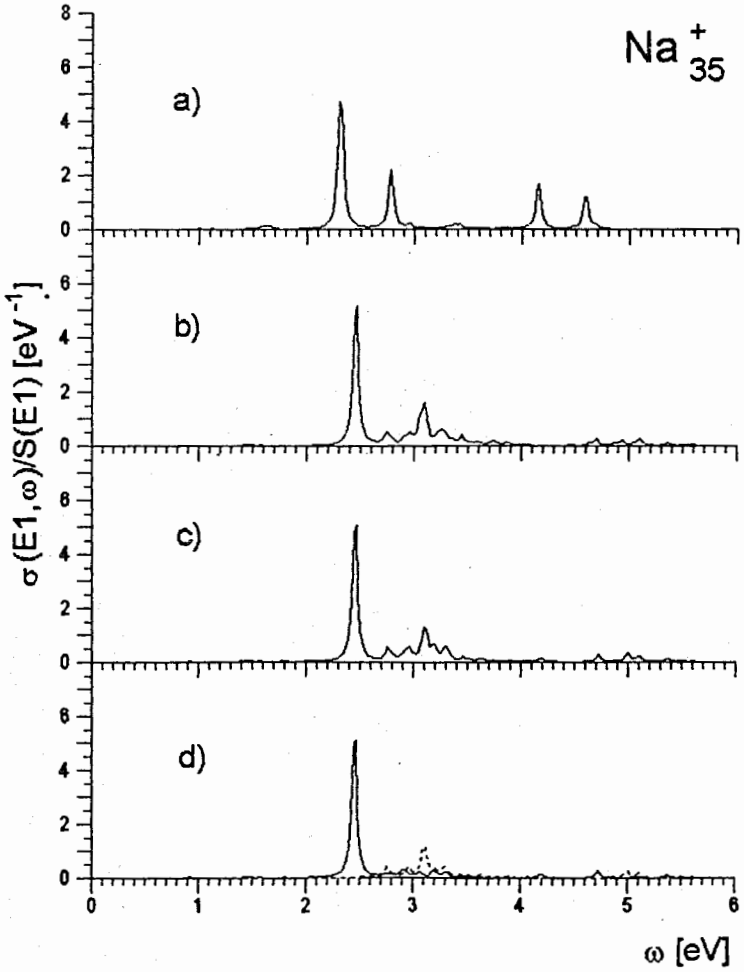

Fig.4. The same as in Fig. 2 for Na_{35}^{+}.

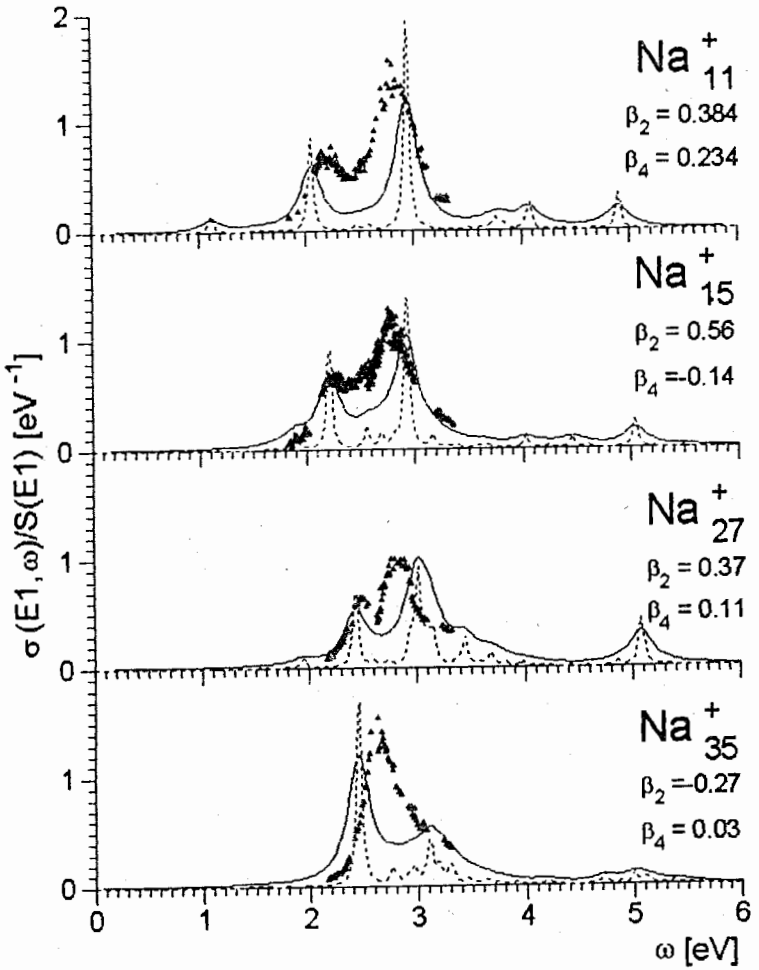

Fig.5. The total normalized E1 strength functions calculated with the small ($\Delta = 0.05eV$, dashed curve) and large ($\Delta = 0.25eV$, solid curve) averaging against the experimental data [22,27] (triangles). For $\Delta = 0.05$ the strength function is decreased by a factor of 3. The calculations use the SAJM deformation parameters [35].

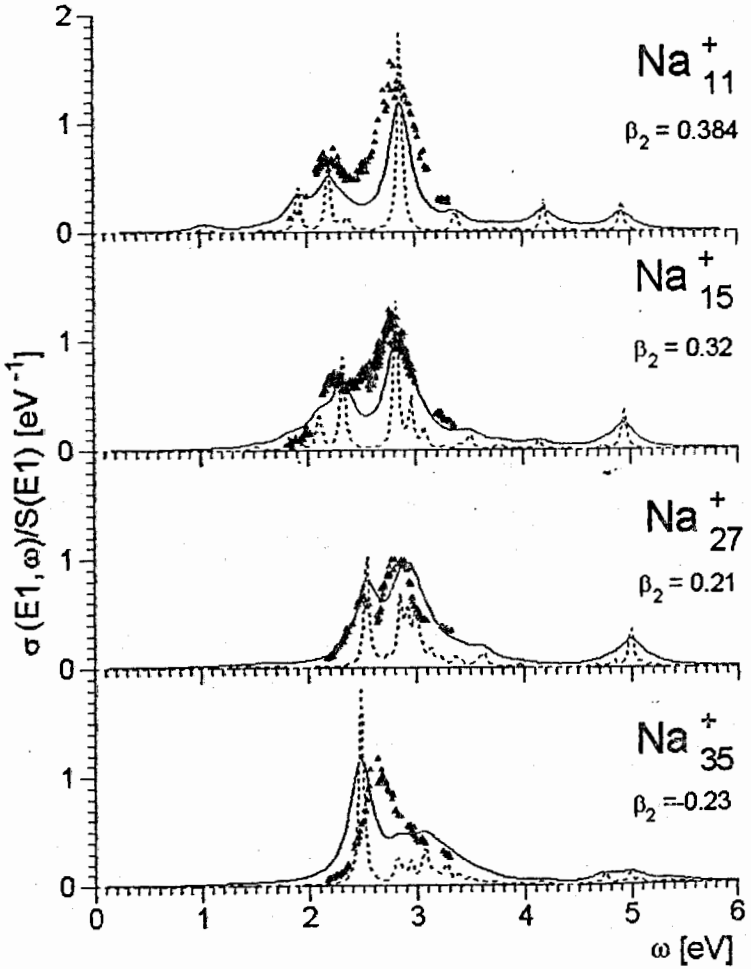

Fig.6. The same as in Fig.5 but with the deformation parameters extracted from [22,27].

Table 2: Experimental [18,22,27] and calculated within the SRPA energy centroids (eV) of the dipole plasmons with projections $\mu = 0$ and 1. The SRPA results have been obtained with the deformation parameters calculated within the SAJM [35] and extracted from the experimental data [22,27]. See the comments in the text.

	Exper.				SRPA			
	[18]		[22,27]		β_2 and β_4 from [35]		β_2 from [22,27]	
	ω	$\Delta\omega$	ω	$\Delta\omega$	ω	$\Delta\omega$	ω	$\Delta\omega$
Na_{11}^+	-	-	2.18, 2.80	0.62	2.05, 2.94	0.89	2.10, 2.84	0.74
Na_{15}^+	2.20(8), 2.77(2)	0.57	2.26, 2.78	0.52	2.22, 2.92	0.70	2.32, 2.83	0.51
Na_{27}^+	2.42(1), 2.83(1)	0.41	2.48, 2.82	0.34	2.44, 3.02	0.58	2.52, 2.92	0.40
Na_{35}^+	2.56(1), 2.87(2)	0.31	2.60, 2.94	0.34	2.45, 3.12	0.67	2.48, 2.88	0.40

Table 2 also demonstrates a good agreement of the SRPA results with the experimental data. The single exclusion is a systematic overestimation of the plasmon deformation splitting $\Delta\omega$ while using the SAJM deformation parameters [35]. Like many other models (see, review in [12]), the SAJM gives β_2 values much larger than the experimental ones. Nevertheless, the local RPA well describes the plasmon deformation splitting with the SAJM deformation parameters [36]. As has been shown above, the calculations with the Woods-Saxon potential reproduce the inertia-tensor diagonal elements and other values which are sensitive to the deformation. However, these calculations have used only single-particle wave functions but not energies, thus not providing a comparison of the single-particle spectrum in deformed Kohn-Sham and Woods-Saxon potentials. In principle, the influence of the deformation on the dynamical response within the local RPA and SRPA could also be somewhat different. Unfortunately, there are no systematic calculations for deformed clusters within other

theoretical models to come into more sight with this problem.

4 Conclusions

The RPA model with the separable self-consistent residual interaction (SRPA) has been applied to describe the dipole plasmon in singly charged deformed sodium clusters, and quite appropriate agreement with the available experimental data is achieved. For the moment, the application of the full RPA to deformed clusters is limited to the simplest case of Na_{10} [6]. The local RPA has successfully been used for deformed clusters with $N_e < 60$ [23] but this model does not describe the Landau damping. So, the SRPA now seems to be a single RPA method which can describe the dipole oscillations in deformed sodium clusters, taking into account the Landau damping and not needing for this aim a large computational effort.

Acknowledgement. We are grateful to M.Brack and P.-G.Reinhard and to Th.Hirschmann for numerous fruitful discussions and communicating results prior to publication. We thank H.Haberland and M.Schmidt as well as J.Borggreen and H.D.Rasmussen for presenting experimental data for the comparison with the results of our calculations and V.V.Gudkov, N.Lo Iudice and J.Kvasil for useful discussions. The work was partly supported by INTAS grant 0151 (V.O.Nesterenko).

APPENDIX

The coefficients used in expression (13) have the following form:

$$N_{\lambda Ll}^{(k)} = (p_k + \lambda + 1)\sqrt{\lambda(2\lambda-1)}(B_{\lambda Ll}^{(1)} - A_{\lambda Ll}^{(1)})$$

$$-(\lambda - p_k)\sqrt{(\lambda+1)(2\lambda+3)}(B_{\lambda Ll}^{(2)} - A_{\lambda Ll}^{(2)}),$$

$$M^{(k)}_{\lambda L l} = (p_k+\lambda+1)\sqrt{\lambda(2\lambda-1)}((l+1)B^{(1)}_{\lambda L l} + lA^{(1)}_{\lambda L l})$$
$$+(\lambda-p_k)\sqrt{(\lambda+1)(2\lambda+3)}((l+1)B^{(2)}_{\lambda L l} + lA^{(2)}_{\lambda L l})$$
$$+(\lambda-p_k)(p_k+\lambda+1)\sqrt{(2\lambda+1)(2l+1)}C^{L0}_{l0\lambda 0}$$

where

$$A^{(1)}_{\lambda L l} = \sqrt{(l+1)(2l+3)}\begin{pmatrix} l+1 & \lambda-1 & L \\ \lambda & l & 1 \end{pmatrix}\cdot C^{L0}_{l+10\lambda-10},$$

$$A^{(2)}_{\lambda L l} = \sqrt{(l+1)(2l+3)}\begin{pmatrix} l+1 & \lambda+1 & L \\ \lambda & l & 1 \end{pmatrix}\cdot C^{L0}_{l+10\lambda+10},$$

$$B^{(1)}_{\lambda L l} = \sqrt{l(2l-1)}\begin{pmatrix} l-1 & \lambda-1 & L \\ \lambda & l & 1 \end{pmatrix}\cdot C^{L0}_{l-10\lambda-10},$$

$$B^{(2)}_{\lambda L l} = \sqrt{l(2l-1)}\begin{pmatrix} l-1 & \lambda+1 & L \\ \lambda & l & 1 \end{pmatrix}\cdot C^{L0}_{l-10\lambda+10}.$$

REFERENCES

1. V.V.Kresin, Phys.Rep. **220**, 1 (1992).
2. V.O.Nesterenko, Sov.J.Part.Nucl. **23**, 1665 (1992).
3. W.A. de Heer, Rev.Mod.Phys. **65**, 611 (1993).
4. M.Brack, Rev.Mod.Phys. **65**, 677 (1993).
5. C.Brechignac and J.P.Connerade, J.Phys. B**27**, 3795 (1994).
6. W.Ekardt and Z.Peznar, Phys. Rev. B**43**, 1322 (1991).
7. J.M.Pacheco and W.Ekardt, Ann. Phys. (Leipzig) **1** 254 (1992).
8. E.Lipparini and S.Stringari, Z.Phys. D**18**, 193 (1991).
9. C.Yannouleas, E.Vigezzi, and R.A.Broglia, Phys.Rev. B**47**, 9849 (1993).

10. C.Yannouleas, F.Catara and N. Van Giai. Phys.Rev. B**51**. 4569 (1995).
11. M.Madjet, C.Guet and W.R.Johnson. Phys.Rev. A**51**. 1327 (1995).
12. Th.Hirschmann, M.Brack and J.Mejer. Annalen Physik **3**. 336 (1994).
13. V.O.Nesterenko, in *Proc. 2nd Intern. Conf. on Atomic and Nuclear Clusters, Santorini, Greece, 1993* (Springer-Verlag. Berlin. 1994). ed. G.S.Anagnostatos and W. von Oertzen, p.256.
14. V.O.Nesterenko and W.Kleinig, Phys.Scr. **T56**. 284 (1995).
15. V.O.Nesterenko W.Kleinig and V.V.Gudkov, Z.Phys. D**34** 271 (1995).
16. V.O.Nesterenko, W.Kleinig, V.V.Gudkov, N. Lo Iudice and J.Kvasil. Preprint JINR E17-96-325, Dubna, 1996; submitted to Phys.Rev.A.
17. K.Selby, M.Vollmer, J.Masui, V.Kresin, W.A. de Heer and W.D.Knight. Phys.Rev. B**40**, 5417 (1989).
18. J.Borggreen, P.Chowdhury, N.Kebaili, L.Lundsberg-Nielsen. K.Lutzenkirchen, M.B.Nielsen, J.Pedersen and H.D.Rasmussen. Phys. Rev. B**48**, 17507 (1993).
19. P.Meibom, M.Østergård, J.Borggreen, B.Bjørnholm and H.D.Rasmussen, to be published in Proc. 8th Int. Symp. on Small Particles and Inorganic Clusters, Copenhagen, 1996.
20. C.Brechignac, P.Cahuzak, F.Carlier, M. de Frutos and J.Leygnier. Z.Phys. D**19**, 1 (1991).
21. Th.Reiners, Ch.Ellert, M.Schmidt and H.Haberland. Phys.Rev.Let. **74**, 1558 (1995).
22. Ch.Ellert, M.Schmidt, Ch.Schmidt, Th.Reiners and H.Haberland. Phys. Rev. Let. **75**, 1731 (1995).

23. Th.Hirschmann et al, to be published in in Proc. 8th Int. Symp. on Small Particles and Inorganic Clusters, Copenhagen, 1996.

24. D.J.Row, *Nuclear Collective Motion* (Methuen, London, 1970) ch. 4, 14-16.

25. A.Bohr and B.Mottelson, *Nucklear Structure* (W.A. Benjamin Inc., New-York, Amsterdam, 1974) v.2, ch.6.

26. P.Ring and P.Schuck, *The Nuclear Many-Body Problem* (Springer-Verlag, Heidelberg, 1980) ch. 8,12.

27. M.Schmidt, H.Haberland et al, to be published.

28. O.Gunnarson and B.I.Lundqvist, Phys.Rev. **B13**, 4274 (1974).

29. M.Brack, Phys.Rev. **B39**, 3533 (1989).

30. P.-G.Reinhard, M.Brack, and O.Genzken, Phys.Rev. **A41**, 5568 (1990).

31. P.-G.Reinhard and Y.K.Gambhir, Ann. Physik, **1**, 598 (1992); P.-G.Reinhard, Ann. Physik, **1**, 632 (1992).

32. W.D.Myers, W.J.Swiatecki, T.Kodama, L.J.El-Jaik and E.R.Hilf, Phys. Rev. **C15**, 2032 (1977).

33. S.V.Tolokonnikov and S.A.Fayans, JETF Lett. **35**, 403 (1982).

34. V.O.Nesterenko, W.Kleinig, V.V.Gudkov and J.Kvasil, Phys.Rev. **C53**, 1632 (1996).

35. Th.Hirschmann, B.Montag and J.Mejer, Z.Phys. **D37**, 63 (1996).

36. Th.Hirschmann, private communication.

Received by Publishing Department on December 15, 1996.

Нестеренко В.О., Клейниг В. E17-96-466

RPA описание дипольных осцилляций
в деформированных патриевых кластерах

В рамках метода хаотических фаз с самосогласованными остаточными силами (SRPA) исследованы дипольные осцилляции валентных электронов в деформированных атомных кластерах патрия. Учтена связь возбуждений поверхностного и объемного типа. Изучено влияние октупольных возбуждений, имеющее место в деформированных системах. Результаты расчетов находятся в хорошем согласии с экспериментальными данными.

Работа выполнена в Лаборатории теоретической физики им. Н.Н.Боголюбова ОИЯИ.

Препринт Объединенного института ядерных исследований. Дубна, 1996

Nesterenko V.O., Kleinig W. E17-96-466

RPA Description of Dipole Oscillations
in Deformed Sodium Clusters

Dipole oscillations of valence electrons in deformed sodium clusters are described within the random-phase-approximation method with the self-consistent separable residual forces (SRPA). The coupling of surface and volume modes is taken into account. The influence of octupole excitations taking place in deformed systems is also considered. The results obtained are in remarkable agreement with available experimental data.

The investigation has been performed at the Bogoliubov Laboratory of Theoretical Physics, JINR.

Preprint of the Joint Institute for Nuclear Research. Dubna, 1996